Journal of Engineering Science *Vol. XXXI, no. 3 (2024), pp. 96 - 116*
Fascicle *Architecture, Civil and Environmental Engineering* *ISSN 2587-3474*
Topic *Environmental Engineering* *eISSN 2587-3482*

https://doi.org/10.52326/jes.utm.2024.31(3).09
UDC 66.021.2.081.3:546.766:628

EVALUATING THE ADSORPTION POTENTIAL OF SUGARCANE BAGASSE AND LEMONGRASS FOR CHROMIUM (VI) REMOVAL IN WASTEWATER TREATMENT

Aminu S. Dangamba [1,2], ORCID: 0009-0001-7709-1524,
Toyese Oyegoke [1,2]*, ORCID: 0000-0002-2026-6864,
Favour E. Ocheje[1,2], ORCID: 0009-0004-5831-857X,
Mahmud A. Dikko [1], ORCID: 0009-0007-0827-5032,
Mohammed S. Galadima [1], ORCID: 0009-0000-1144-9549

[1] Chemical Engineering Department, Ahmadu Bello University Zaria, Nigeria.
[2] Green Science Promoters' Forum of Pencil Team, Ahmadu Bello University Zaria, Nigeria.
* Corresponding author: Toyese Oyegoke, *OyegokeToyese@gmail.com*

Received: 08. 15. 2024
Accepted: 09. 24. 2024

Abstract. The increasing levels of chromium (VI) ions in textile wastewater pose significant environmental challenges, necessitating effective treatment methods. This study evaluates the biosorption potential of sugarcane bagasse (SCB) and lemongrass (LM), both individually and in blend form, for the removal of chromium (VI) ions. Batch adsorption experiments were conducted to assess the impact of contact time and adsorbent dosage on removal efficiency. BET analysis revealed that the blend had the highest surface area (1047.885 m^2/g), enhancing its adsorption capacity, while FTIR spectroscopy identified key functional groups such as hydroxyl and carbonyl that facilitate metal binding. Results indicated that the blend exhibited superior adsorption capacity, with kinetic studies showing that the adsorption process followed a Pseudo-second order model, suggesting chemisorption as the dominant mechanism. Isotherm analyses indicated that the Langmuir model best-described adsorption on SCB, while the Freundlich model was more suitable for LM and the blend. This research recommends the practical application of SCB and LM in wastewater treatment and encourages further investigation into their potential for removing other heavy metals, highlighting a sustainable approach to environmental remediation.

Keywords: *Chromium, Biosorption, Sugarcane, Bagasse, Lemongrass, Wastewater, Adsorption*.

Rezumat. Nivelurile crescânde de ioni de crom (VI) în apele uzate din industria textilă reprezintă provocări semnificative de mediu, necesitând metode eficiente de tratare. Acest studiu evaluează potențialul de biosorbție al borhotului de trestie de zahăr (SCB) și lemongrass (LM), atât individual, cât și sub formă de amestec, pentru îndepărtarea ionilor de crom (VI). A fost efectuată adsorbția în loturi pentru a evalua impactul timpului de contact și al dozei de adsorbant asupra eficienței de îndepărtare. Analiza BET a arătat că amestecul a avut cea mai mare suprafață (1047,885 m^2/g), sporind capacitatea sa de adsorbție, în timp ce spectroscopia FTIR a identificat grupuri funcționale cheie, cum ar fi hidroxil și carbonil, care facilitează legarea metalelor. Rezultatele au indicat că amestecul a prezentat o capacitate de

adsorbție superioară, studiile cinetice arătând că procesul de adsorbție a urmat un model de ordinul pseudo-doi, sugerând chimisorbția ca mecanism dominant. Analiza izotermelor a indicat că modelul Langmuir a descris cel mai bine adsorbția pe SCB, în timp ce modelul Freundlich a fost mai potrivit pentru LM și amestec. Această cercetare recomandă aplicarea practică a SCB și LM în tratarea apelor uzate și încurajează investigarea ulterioară a potențialului lor de îndepărtare a altor metale grele, evidențiind o abordare durabilă a remedierii mediului.

Cuvinte cheie: *crom, biosorbție, trestie de zahăr, borhot, lemongrass, ape uzate, adsorbție.*

1. Introduction

Water pollution has become one of the most critical environmental challenges, largely due to the discharge of toxic and hazardous chemicals from industrial activities [1]. As industrial development accelerates, substantial amounts of wastewater and domestic sewage containing metal ions are released into water bodies worldwide, significantly contributing to water pollution [2]. Metals released from industries such as tanning, sewage treatment, refining, pharmaceuticals, and textiles accumulate in soil ecosystems, adversely affecting the diversity, density, and physiological functioning of soil microbes [3]. Among numerous heavy metal pollutants, cadmium (Cd), lead (Pb), mercury (Hg), arsenic (As), and chromium (Cr) have been identified as top priorities due to their high toxicity and significant implications for public health [4]. Notably, chromium exists primarily in two forms: trivalent Cr (III) and hexavalent Cr (VI). The relationship between these forms is significantly influenced by environmental pH and oxidative characteristics. Public concern centers particularly on Cr (VI) ions, which is 100 times more hazardous than Cr (III) ions and poses serious health risks due to its carcinogenic, mutagenic, and teratogenic properties. The U.S. Environmental Protection Agency (EPA) has established a limit of 0.05 mg/L for Cr (VI) in drinking water, while the maximum allowable concentration in industrial wastewater is set at 0.1 mg/L [5].

To protect environmental and public health, it is essential to eliminate heavy metals, commonly used in various industries, from water and wastewater through effective treatment techniques. Several control technologies have been developed to treat metal-contaminated water, including chemical precipitation, ion exchange, membrane filtration, coagulation-flocculation, and solvent extraction. However, these methods face challenges such as high operational costs, significant energy requirements, low efficiency, and the generation of large quantities of toxic sludge [6]. Consequently, there is an urgent need for more viable and sustainable approaches to remove heavy metals from wastewater.

Among these methods, biosorption has gained attention as a promising alternative due to its advantages, including the regeneration of biosorbents, potential for metal recovery, minimization of toxic sludge, high removal efficiency, and low operational costs. Biosorption is a physiochemical process that occurs naturally in certain biomass, allowing these materials to passively concentrate and bind pollutants onto their cellular structures. While the application of biomass in environmental cleanup has been established for some time, researchers and engineers aim to harness this phenomenon as an economical solution for removing toxic heavy metals from industrial wastewater [7]. Recent studies have investigated various biomass-based adsorbents, including cyanobacterial biomass [8], *Streptomyces rimosus* [9], peanut husk [10], eucalyptus bark [11], sugarcane bagasse (SCB), and orange peel composites [12], as well as *Eucalyptus tereticornis* composites [13] for effectively removing heavy metals from wastewater.

Sugarcane, SCB (*Saccharum officinarum*) is a lignocellulosic tropical plant extensively cultivated in regions such as Brazil, India, China, Mexico, and South Africa, making it a vital component of the global sugar industry [14]. Following sugar extraction through chewing or refining, large quantities of bagasse are produced, which is often incinerated for energy generation. Sugarcane bagasse consists of approximately 46% cellulose, 24.5% hemicellulose, and 19.95% lignin [15]. The biosorbents derived from SCB contain various functional groups, including –COOH, -OH, -NH2, -OCH3, and –SH, facilitating the attraction and binding of pollutants through chelation, complexation, coordination, and hydrogen bonding [16].

Lemongrass (LM), scientifically known as *Cymbopogon citratus*, is a perennial grass that can grow up to 1.5 meters tall, with multiple stiff stems arising from rhizomatous rootstock. Commonly used in local cuisine and in the manufacture of soap and candles due to its citrus scent, lemongrass belongs to the Cymbopogon section of the *Andropogoneae* in the family *Poaceae*. It contains various compounds, including terpenes, flavonoids, and alkaloids, depending on its habitat. The oil extracted from lemongrass has been utilized to treat various ailments, including coughs, colds, rheumatism, digestive issues, bladder problems, and as a mouthwash for toothaches and sore gums [17]. Additionally, lemongrass (LM) serves as a biosorbent due to its functional groups, such as carbonyl, carboxyl, and hydroxyl, which facilitate the removal of hazardous pollutants [18].

Given their unique chemical compositions and availability, SCB and LM were selected as representative biosorbents for this study. To the best of the author's knowledge, no data have been published on the removal of Cr (VI) ions using SCB and LM individually or in combination. The primary aim of this study is to evaluate the performance of SCB, LM, and their blend in removing Cr (VI) ions from textile wastewater. The effects of contact time and adsorbent dosage on adsorption capacity will be determined using batch systems, and the optimal conditions for Cr (VI) ions removal will be assessed through Response Surface Methodology (Central Composite Design) utilizing Design Expert version 13. The biosorption data will be analyzed and reported using various equilibrium isotherm and kinetic models.

2. Materials and methods

2.1. *Materials and Chemicals*

In this study, all materials and chemicals were of commercial and analytical grade purity, purchased from BDH Chemicals Ltd. (Poole, England), and were used without further purification. Aquatron A4000 distilled water was utilized for standardization and preparation of all samples to mitigate potential interference from other ions and impurities. The equipment employed included a magnetic stirrer, beakers, filter paper, and sample bottles.

2.2. *Collection of Wastewater*

This research focused on two natural and renewable lignocellulosic fibers. Sugarcane bagasse was collected from a sugarcane juice vendor on the Ahmadu Bello University campus in Zaria, while lemongrass was harvested in Funtua Town, Katsina State, Nigeria. Both biomasses were identified at the Herbarium section of the Biological Science Department at Ahmadu Bello University, Zaria, Kaduna, Nigeria. The sugarcane bagasse (SCB) and lemongrass (LM) were meticulously washed with tap water followed by distilled water to eliminate adhering dirt and other particulate matter. The cleaned biomasses were dried at room temperature and then in an oven at 65°C until a consistent weight was achieved. The

dried biomass was finely crushed into a powder and sieved to a particle size of ⩽ 1.44 mm. The fine powder was immersed in 0.1 M NaOH for 24 hours to remove impurities, increase the surface area of the biosorbent, and activate more functional groups. After 24 hours, the biosorbents were thoroughly rinsed with distilled water until a neutral pH was obtained. The NaOH-treated biomass was further dried in an oven at 45°C for 6 hours and stored in sealed polythene bags for subsequent use.

2.3. *Collection and Preparation of Biosorbent*

Samples were collected from wastewater discharges originating from the textile industry using a ten-liter plastic jerry can. Collection occurred between 9 AM and 1 PM, representing peak flow periods due to high production levels. The samples were transported to the laboratory for heavy metal and biosorption studies, with pH and temperature measured at the point of collection.

2.4. *Characterization of Biosorbents*

The surface area, pore size distribution, and pore volume were measured using the Brunauer-Emmett-Teller (BET) analysis method, based on nitrogen adsorption-desorption at liquid nitrogen temperature, conducted with Quantachrome NovaWin version 11.3. The surface morphology of both loaded and unloaded SCB, LM, and their composites was examined before and after Cr (VI) uptake using Scanning Electron Microscopy (SEM, Thermo Scientific Quanta 650). The existing chemical functional groups involved in the biosorption of Cr (VI) onto SCB, LM, and their blend were detected by Fourier Transform Infrared (FTIR) spectroscopy (240FS, Agilent) before and after uptake, with samples analyzed in the range of 4000-500 cm^{-1} at room temperature.

2.5. *Batch Sorption Experiment*

2.5.1. Optimization Conditions for Biosorption

The optimum conditions for the biosorption of Cr (VI) ions onto SCB, LM, and their blend were determined using Central Composite Design (CCD). CCD is commonly employed under Response Surface Methodology (RSM) due to its suitability for fitting quadratic surfaces. It involves a combination of factorial points, center points, and axial points, which are effective for process optimization. Optimization studies investigated the effects of experimental factors, such as contact time and adsorbent dosage, on the adsorption capacity of Cr (VI) ions using SCB, LM, and their blend. The effect of contact time was explored within the range of 20-120 min, while the effect of adsorbent dosage was studied within the range of 0.1-0.9 g.

2.5.2. Biosorption Experiment

Batch experiments were carried out in 50 mL beakers. A specific amount of SCB, LM, and their blend, according to the design formulation of CCD, was added to 25 mL of the Cr (VI) wastewater solution. The resulting solutions were stirred vigorously with a magnetic stirrer at 150 rpm for a predetermined period until equilibrium was reached. After equilibrium was achieved, the biomasses were separated from the solutions using Whatman filter paper, and the concentration of the supernatant was determined using Atomic Absorption Spectrometry (AAS). The quantity of metals adsorbed was calculated using Equation 1:

$$q_e = \frac{C_0 - C_f}{m} V \quad (1)$$

where: q_e is the adsorption capacity (mg/g), C_o and C_e are the initial and equilibrium concentration (mg/L) of metal ions, respectively. V and m represent the solution volume and mass (g) of the adsorbent respectively.

2.6. *Equilibrium Adsorption Isotherm Models*

Adsorption isotherms describe the equilibrium relationship between the quantity of sorbate (metal ions) sorbed by the biosorbent and the concentration in the equilibrium solution at constant temperature [4]. They provide valuable information regarding the mechanism and nature of the adsorption process and facilitate the evaluation of the feasibility of the adsorption process for a given application. In this work, commonly used isotherm models, including Langmuir, Freundlich, and Temkin, were employed to interpret Cr (VI) ions sorption and understand the mechanism of biosorption on SCB, LM, and their blend. The experimental data were fitted into these equilibrium isotherm models.

2.6.1. Langmuir Isotherm Model

The Langmuir isotherm model is based on the assumption that sorption occurs over energetically homogeneous sites of the biosorbent, resulting in a monolayer coverage. The non-linear form of the Langmuir equation is given in Equation 2:

$$q_e = \frac{q_m b C_e}{1+bC_e} \quad (2)$$

where: C_e is the equilibrium concentration of metal ion (mg/L); q_e is the amount of metal ion adsorbed per unit weight of adsorbent material at equilibrium (mg/g); b is the Langmuir constant (L/mg) which represents the adsorbate's degree of adsorption affinity, and q_m is the maximum adsorption capacity (mg/g) associated with full monolayer cover. The Langmuir isotherm is characterized by essential properties that can be related in terms of a dimensionless separation factor R_L. This factor allows the prediction of the form of adsorption isotherm, providing insights into whether the sorption process is favorable or not. Specifically, the process is considered unfavorable when R_L >1, linear when R_L =1, favorable in the interval 0< R_L<1 and irreversible when R_L =0 [19]. The separation factor R_L can be calculated using equation 3.

$$R_L = \frac{1}{1+bC_0} \quad (3)$$

where: C_o is the initial metal concentration (mg/L) and b is the Langmuir constant.

2.6.2. Freundlich Isotherm Model

The Freundlich isotherm model assumes an exponential decrease in the biosorption energy with increasing surface coverage. It is applicable to heterogeneous surfaces with negligible interactions between sorbed molecules. The model is expressed in Equation 4:

$$q_e = K_f C_e^{1/n} \quad (4)$$

where: C_e is the equilibrium concentration (mg/L); q_e is the amount of metal ion adsorbed per unit weight (mg/g); K_f and n are Freundlich constants indicating the sorption capacity. The favorability of the Freundlich model was determined by n. Values of n in the range of 1-10 indicate favorable adsorption, while n<1 indicates unfavorable adsorption and the parameter $1/n$ is an empirical factor that relates to the biosorption intensity [20].

2.6.3. Temkin Isotherm Model

The Temkin isotherm model assumes a uniform distribution of binding energies over a number of adsorption sites [21]. The non-linear form of the Temkin is represented in Equation 5:

$$q_e = \frac{RT}{b_T} In(K_T C_e) \quad (5)$$

where: $B = \frac{RT}{b_T}$ with the universal gas constant, R = 8.314 J/mol.K, and T as the absolute temperature in Kelvin; b_T is the Temkin isotherm constant; q_e (mg/g) is the amount of metal ions absorbed onto the adsorbent at equilibrium. The Temkin parameters A and B are the equilibrium binding energy and constant heat of sorption respectively.

2.7. *Adsorption Kinetic Models*

Analyzing kinetic models in biosorption studies is critical for understanding the reaction pathways, mechanisms, and process dynamics. It aids in determining the physiochemical interactions, mass transport, and rate-determining phases in the biosorption process. Additionally, understanding the kinetics of metal sorption is essential for optimizing sorption processes, reactor dimensions, and residence times [6]. Therefore, to evaluate the rate and mechanism of metal biosorption, the experimental kinetic data were analyzed using various reaction rate and diffusion models, including the Pseudo-first-order, Pseudo-second-order, and Elovich kinetic models.

2.7.1. Pseudo-First-Order Kinetic Model

The Pseudo-first-order (PFO) kinetic model, proposed by Lagergren (1898), is based on the assumption that the sorption rate is proportional to the number of free available sites (Lee et al., 2014). It is typically employed to analyze kinetic behavior at the initial stages of the biosorption process, and its non-linear form is expressed in Equation 6:

$$q_t = q_e(1 - e^{-k_1 t}) \quad (6)$$

where: k_1 is the PFO rate constant (min^{-1}); q_t and q_e are the amount of metal ion sorbed at time t and at equilibrium (mg/g), respectively.

2.7.2. Pseudo-Second-Order Kinetics

The Pseudo-second-order (PSO) model assumes that chemical reactions occur between the metal ions and the biosorbent, resulting in the formation of strong covalent bonds [14]. The non-linear PSO kinetic model is mathematically represented by Equation 7:

$$q_t = \frac{k_2 q_e^2 t}{1 + k_2 q_e} \quad (7)$$

where: k_2 is the PSO rate constant in $\mathrm{g/(mg/min)}$, qt and q_e are the amount of metal ion adsorbed at time (t), and at equilibrium in $\mathrm{mg/g}$, respectively.

2.7.3. Elovich Kinetic Model

The Elovich kinetic model, which considers the surface as energetically heterogeneous, is frequently employed to interpret adsorption kinetics. It effectively describes second-order kinetics and was originally developed to explain the kinetics of gas chemisorption on solids [22]. The Elovich kinetic model can be expressed in Equation 8:

$$q_t = \frac{1}{b}\ln(ab) + \frac{1}{b}\ln(t) \quad (8)$$

where: a is the initial adsorption rate in $\mathrm{mg/(g{\cdot}min)}$ and *b* is the constant.

2.8. *Statistical Analysis*

In general, the data were fitted into the respective models to obtain corresponding slopes and intercepts from the plot of q_t versus ln(t), by non-linear regression method using R-square values to ascertain to the suitability of the model to fit the adsorption experiment data.

3. Results and discussions

3.1. *Characterization of the Biosorbent*

3.1.1. Analysis of Brunauer-Emmet-Teller (BET)

The quality of biosorbents is strongly indicated by a high surface area as it correlates directly with the adsorption capacity. The Brunauer-Emmett-Teller (BET) technique was employed to quantify the surface area, pore diameter, and pore volume [23]. The average values for BET surface area, total pore volume, and pore size for SCB, LM and their blend are provided in Table 1. For SCB, the surface area, pore volume, and pore size were determined to be 501.999 m^2/g, 0.253 cm^3/g and 2.10 nm, respectively. These values were discovered to be considerably higher reported by [24] and [25], with the exception of the pore size, which closely aligned with the findings of [25]. LM exhibited a specific surface area of 811.761 m^2/g, a pore volume of 0.406 cm^3/g and a pore size of 2.125 nm. These values were in accordance with the findings of [26]. Comparatively, the blend of SCB and LM demonstrated a higher surface area and pore volume, measuring 1047.885 m^2/g and 0.544 cm^3/g, respectively. This implies that the composite may possess enhanced metal adsorption capabilities and increased metal uptake, attributed to its larger surface area [12].

Table 1

Biosorbent surface area, pore volume, pore diameter

Biosorbent	BET Surface area (m^2/g)	Pore volume (cm^3/g)	Pore size (nm)
Sugarcane bagasse	501.999	0.253	2.100
Lemongrass	811.761	0.406	2.125
Blend	1067.885	0.544	2.105

3.1.2. Analysis of the Fourier Transform Infrared (FTIR) Spectra

The FTIR spectra of SCB, LM and their blend before and after Cr (VI) uptake were studied to qualitatively determine the major functional groups on the surface of the adsorbent. The spectral analysis covered a wavelength range from 4000 to 500 cm^{-1} as shown in Figures 1 and 2 for SCB, LM and their blend respectively. The infrared (IR) spectrum obtained from FTIR of SCB displayed a number of different absorption peaks. Distinct peaks were identified in the FTIR spectra of SCB, specifically at 3292, 2906, 1603, 1379, 1259, 1036, and 916 cm^{-1}. The peak at 3292 cm^{-1} corresponds to the O-H stretching of hydroxyl groups in Cellulose I, as reported by [27]. The presence of peak at 2906 cm^{-1} indicates C-H stretching of alkane groups, while the increased intensity at 1603 cm^{-1}, associated with C=O stretching, suggests the uptake of Cr (VI) metals, potential pollutants in wastewater [14]. The peak at 1512 cm^{-1} is linked to the C=C carboxylic groups of aromatic rings, and the range from 2311 to 1841 cm^{-1} indicates C≡C stretching vibrations of lignin aromatic rings [12]. The intense 1036 cm^{-1} peak represents C-O stretching vibration of cellulose, lignin, and hemicellulose [27]. According to the study, these major functional groups, which include hydroxyl, carbonyl, and aromatic rings, play an important role in Cr (VI) sorption. They are actively involved in binding interactions with metal ions, and the spectral changes imply the creation of metal

complexes. Complexation interactions are seen as the primary driving factor underlying the sorption mechanism, as supported by [14, 27, 28].

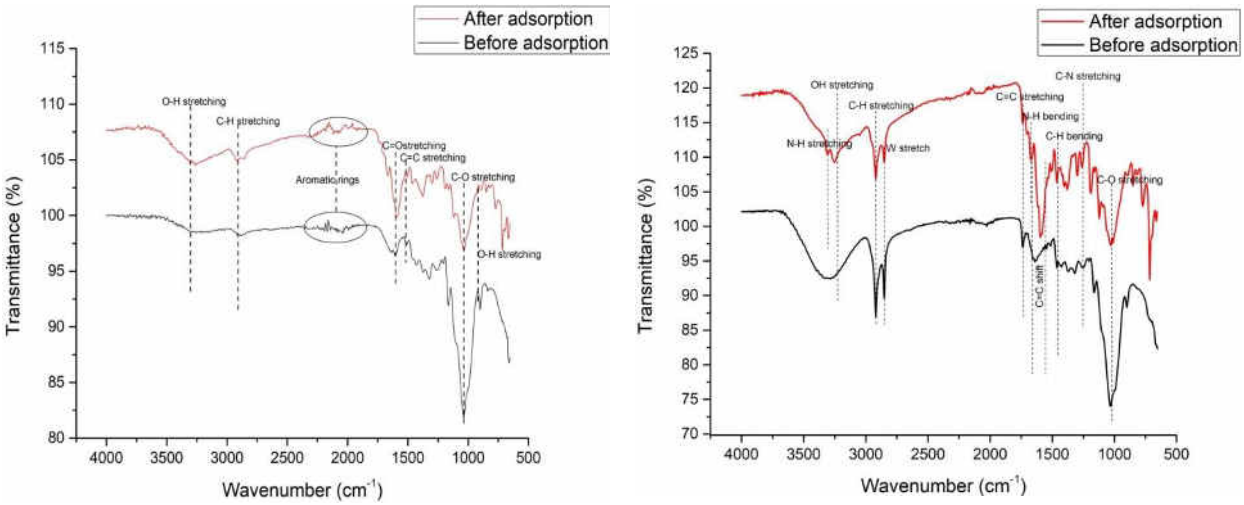

Figure 5. FTIR spectra obtained before and after adsorption of Cr (VI) using sugarcane bagasse (left) and lemongrass (right).

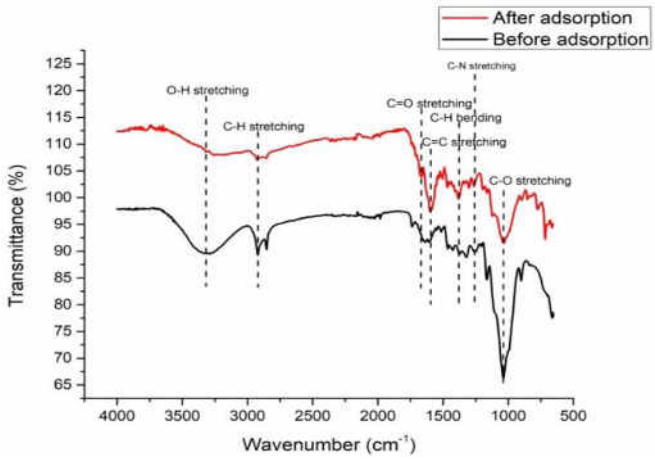

Figure 6. FTIR spectra of a blend derived from SCB and LM before and after adsorption of Cr (VI) ions.

3.1.3. Analysis of the Scanning Electron Microscopy (SEM) Images

Scanning electron microscopy (SEM) analysis was conducted on SCB, LM and their blend before and after the sorption of Cr (VI) ions to examine the resulting changes in the surface morphology. The observed changes are shown in Figures 3, 4 and 5 for SCB, LM and their blend, respectively. The figures illustrate the surface texture and porosity which include wide openings and large pores both before and after Cr (VI) ions uptake. The uneven surfaces are attributed to the presence of parallel grooves and cracks, and granules with irregularly shaped cavities and voids. The rough and porous surface before sorption may offer possible sorption sites for the uptake of Cr (VI) ions [29]. The analysis of surface morphology indicates that SCB exhibits larger pore sizes before Cr (VI) uptake (Figure 3 (LHS)) compared to SCB after Cr (VI) ions uptake, where fewer pores are observed (Figure 3 (RHS)). This reduction in pore size may be because the pores have been filled due to the uptake of Cr (VI) ions by the SCB [14]. The surface morphology of LM after Cr (VI) ions uptake, as shown in Figure 4 (RHS), reveals significant changes, transforming coarse particle sizes into finer ones, when compared to the rough and uneven surface before Cr (VI) ions uptake in Figure 4 (LHS). These

changes could be as a result of the deposition of Cr (VI) ions onto the surface of LM. Similar observation was reported in the work of [15]. The micrographs surface of the blend material in Figure 5 (LHS) exhibited larger pores, rough and uneven surface because of a hydrolysis reaction occurring on the surface of the blend material [15]. In Figure 5 (RHS), the surface became smoother with less porosity, which is likely attributed to the entrapment of Cr (VI) ions on the surface of the blend material [30].

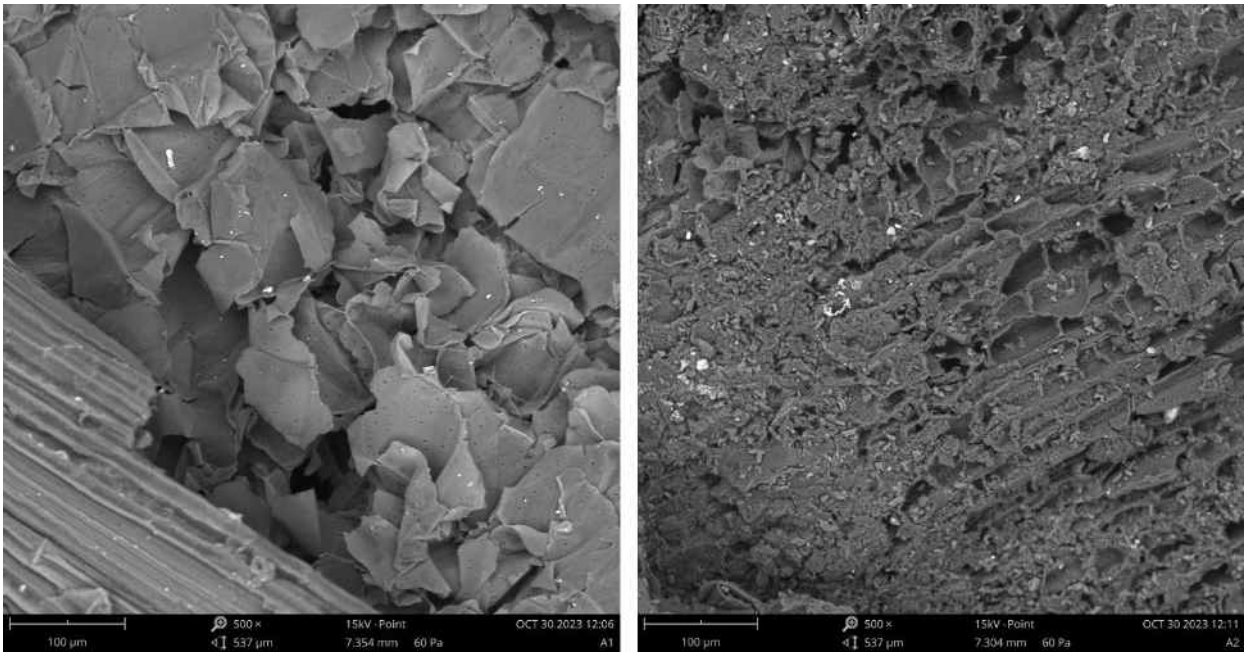

Figure 3. SEM micrographs of sugarcane bagasse before (left) and after (right) Cr (VI) uptake.

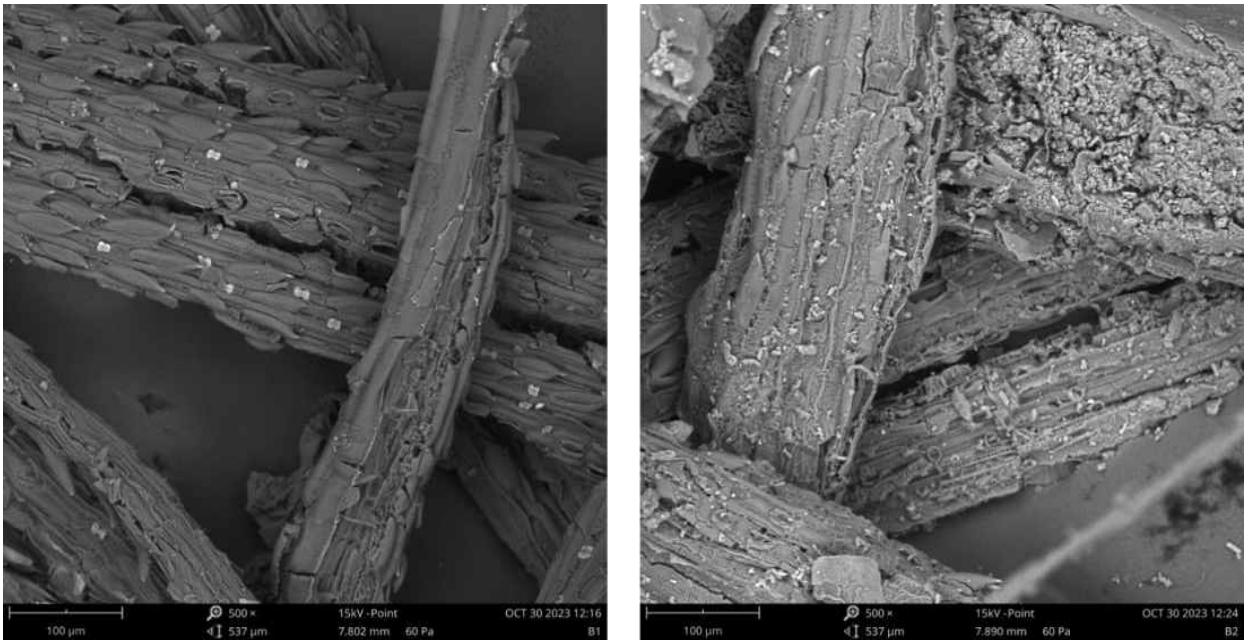

Figure 4. SEM micrographs of lemongrass before (left) and after (right) Cr (VI) uptake.

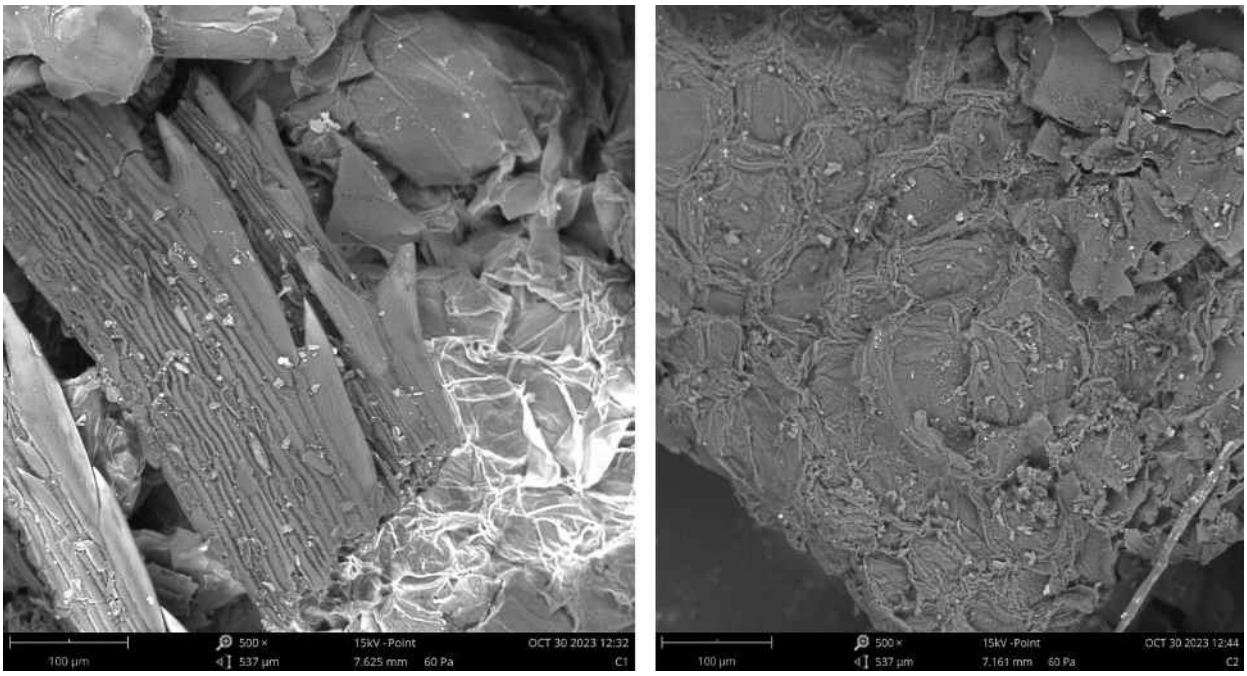

Figure 5. SEM micrographs of a composite derived from SCB and LM before (left) and after (right) Cr (VI) uptake.

3.2. *Optimization studies of the metal removal*

3.2.1. Fitting process model statistical analysis

The optimum level of process parameters, such as contact time and adsorbent dosage were obtained with the CCD experimental design. The interactive effect of contact time and adsorbent dosage on the adsorption capacity was subsequently studied. Statistical software, specifically design expert version 13.5, was used for the regression analysis of the data to evaluate the statistical significance of the quadratic model. The analysis of variance ANOVA for the response surface model of Cr (VI) ions adsorption on SCB, LM and their blend are presented in Table 2. The analysis of variance (ANOVA) results from Table 2 indicates that the analyzed variables fall within an acceptable range. ANOVA was used to verify the quadratic models, revealing the ability to predict Cr (VI) ions uptake. The equations of the models, generated after interpreting the experimental data for the biosorption Cr (VI) ions by SCB, LM and the blend are presented in Equations 9, 10 and 11, respectively.

$$qCr = 0.408865 + 0.003639A + 0.058496B + 0.000778AB - 0.000022A^2 - 0.042756B^2 \quad (9)$$

$$qCr = 1.63198 - 0.007455A - 0.410243B - 0.001238AB + 0.000042A^2 + 0.362925B^2 \quad (10)$$

$$qCr = 0.369950 + 0.010817A + 2.31205B + 0.001132AB - 0.000059A^2 - 2.08442B^2 \quad (11)$$

where: qPb and qCr are the predicted adsorption capacities for Pb (II) and Cr (VI) ions respectively, the actual values of the test variables, contact time and adsorbent dosage are represented by A and B respectively. The coefficient involving two factors, namely (AB) and (A^2 and B^2) signifies the interaction between these two parameters and the quadratic effect. The negative sign in front of the term indicates an antagonistic effect, whereas the positive sign indicates a synergistic effect [31]. The correlation coefficient (R^2) was used to evaluate the model fitness. The closer the R^2 is to 1, the stronger the model and the better it predicts the response [25]. The P and F values indicate the significance of the regression coefficients and the overall significance of the model. The model term is considered significant if the P value is < 0.05 [32]. The results presented in Table 2 showed that the regression was

statistically significant for the adsorption of Cr (VI) ions using SCB, with an F value of 707.49 and prob > F (<0.0001).

Table 2

Summary of the ANOVA results for the adsorption of Cr (VI) ions using SCB, LM and their blend as an adsorbent

Parameters	Sugarcane bagasse	Lemongrass	Composite
Model	<0.0001	<0.0001	<0.0001
Standard deviation	0.0067	0.0101	0.0209
Mean	0.5632	1.25	1.28
Coefficient of variance	1.2000	0.8139	1.63
R^2	0.9898	0.9955	0.9959
Adjusted R^2	0.9825	0.9923	0.9930
Predicted R^2	0.9402	0.9783	0.9791
Adequate precision	33.2072	48.7025	51.7078
Lack of fit	0.1277	0.3357	0.2903

In equation 9, the correlation coefficient R^2 (0.9898) value for the adsorption of Cr (VI) using SCB, was found to be close to 1 and in reasonable agreement with the adjusted correlation coefficient (Adjusted R^2=0.9825), indicating high model significance. While the predicted R^2 (0.9402) is not as high, but the model remains significant.

The term adequate precision (AP) ratio corresponds to the target's response variable under varying noise conditions. An AP value greater than 4 is desirable. The reproducibility of the model is indicated by the coefficient of variance (CV). It is calculated as the ratio of the stand error of the estimate to the mean value of the response. The model is deemed reproducible if the value is less than 10% [31]. The model F-value for the adsorption of Cr (VI) ions was found to be 310.19, implying that the model is significant. Additionally, Prob > F values less than 0.05 indicate that the model terms are significant at 95% confidence level. The R^2 value of Cr (VI) ions was found to be 0.9955, which is close to unity, is desirable and in reasonable agreement with the adjusted R^2 value of 0.9923 for Cr (VI) ions. The term "adequate precision" (AP) ratio refers to the response variable concerning the target under varying noise conditions. The adequate precision (AP) obtained for the adsorption of Cr (VI) ions using LM was found to be 48.7025. An AP value higher than 4 is desirable [31]. The results also from Table 2, for the adsorption of Cr (VI) ions using the blend of SCB and LM indicate that the regression is statistically significant, with an *F* value of 343.43 for Cr (VI) ions, and a prob > F value less than 0.0001. The term is considered significant if the *P* value < 0.05. The R^2 value of Cr (VI) ions was found to be 0.9959, indicating that the values are desirable and are close to unity.

The value of R^2 for Cr (VI) ions (0.9959), and the predicted R^2 of 0.9197 for Cr (VI) ions adsorption are also in good agreement with the adjusted R^2 0.9930. The response variable in respect to the goal under changing noise levels is referred to as the "adequate precision" (AP) ratio.

The adequate precision (AP) for Cr (VI) ion adsorption using a blend from SCB and LM was 51.7078. An AP value greater than 4 is considered desirable [31]. According to the summary of ANOVA results presented in Table 2, the independent variable (contact time and adsorbent dosage) are significant terms for the adsorption of Cr (VI) ions from textile wastewater using SCB, LM and a blend derived from SCB and LM.

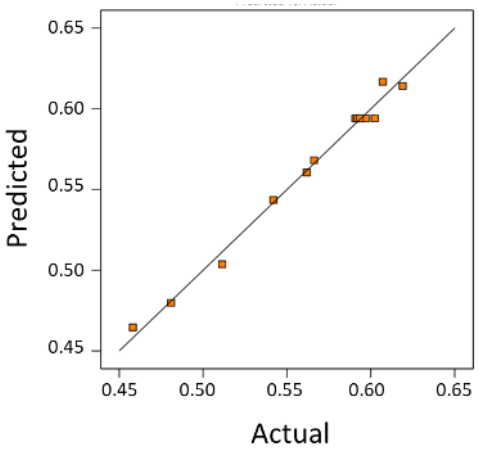

Figure 6. A parity plot showing the actual and predicted values for the adsorption of Cr (VI) ions using SCB as adsorbent.

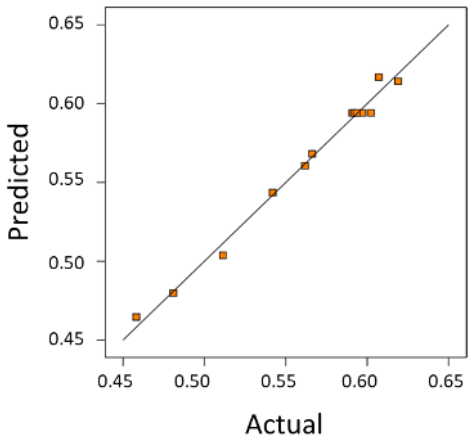

Figure 7. A parity plot showing the actual and predicted values for the adsorption of Cr (VI) ions using LM as adsorbent.

To show the correlation between actual and predicted values, a parity plot is employed to show the relationship for the adsorption of Cr (VI) ions using SCB, LM, and the blend derived from SCB and LM in Figures 6, 7, and 8, respectively. For a model to be reliable, it should accurately predict the response when compared with the experimental data. As shown, there is a significant correlation between the actual and predicted values, suggesting that the generated models successfully capture the relationship between the adsorption variables (contact time and adsorbent dosage) and the metal uptake rate.

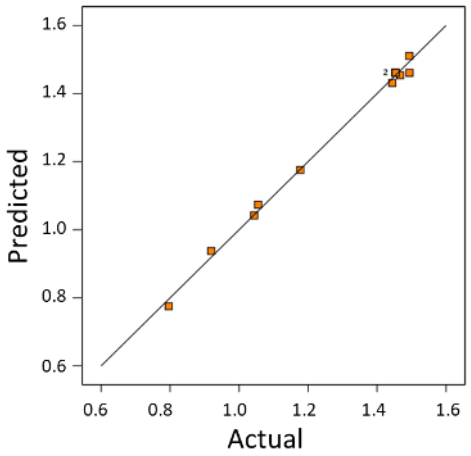

Figure 8. A parity plot showing the actual and predicted values for the adsorption of Cr (VI) ions using a blend derived from SCB and LM as an adsorbent.

The parity plots of SCB, LM, and their blend reveal that the data points cluster around the diagonal line, implying a satisfactory agreement between the predicted and the actual values. This suggests that the models generated successfully capture the relationship between the independent adsorption variables (contact time and adsorbent dosage) and the adsorption capacity. The model for SCB exhibits a high correlation coefficient (R^2) of 0.9898 for Cr (VI) ions adsorption, indicating the suitability and accuracy of the models in predicting the adsorption capacity under variable conditions of contact time and adsorbent dosage. The model equation for Cr (VI) ions is statistically significant, as the Prob. >F values are less than 0.05, and the R^2 value is 0.9898. Similarly, the high correlation coefficient R^2 for LM in the adsorption of Cr (VI) ions indicates the suitability and accuracy of the model, being close to

unity. The closer the R^2 value is to unity, the stronger and better the model predicts the response. Moreover, the high correlation coefficient R^2 of 0.9959 for the adsorption of Cr (VI) ions using the blend further indicates a well-fitted model that can predict the adsorption capacity with reasonable certainty under independent variables such as contact and adsorbent dosage. In conclusion, the parity plots exhibit a satisfactory correlation between the actual and the predicted values for SCB, LM, and the blend derived from SCB and LM.

3.2.2. Effect of Model Variables and Their Interactions

The three-dimensional response surface plots are essential for determining the optimum values of the variables and illustrating the interaction between contact time (A) and adsorbent dosage (B) on the adsorption capacity (q, mg/g) of biosorbent during the adsorption of Cr (VI) ions from textile wastewater using SCB, LM and a blend derived from SCB and LM at room temperature, as presented in Figure 9 and Figure 10, respectively.

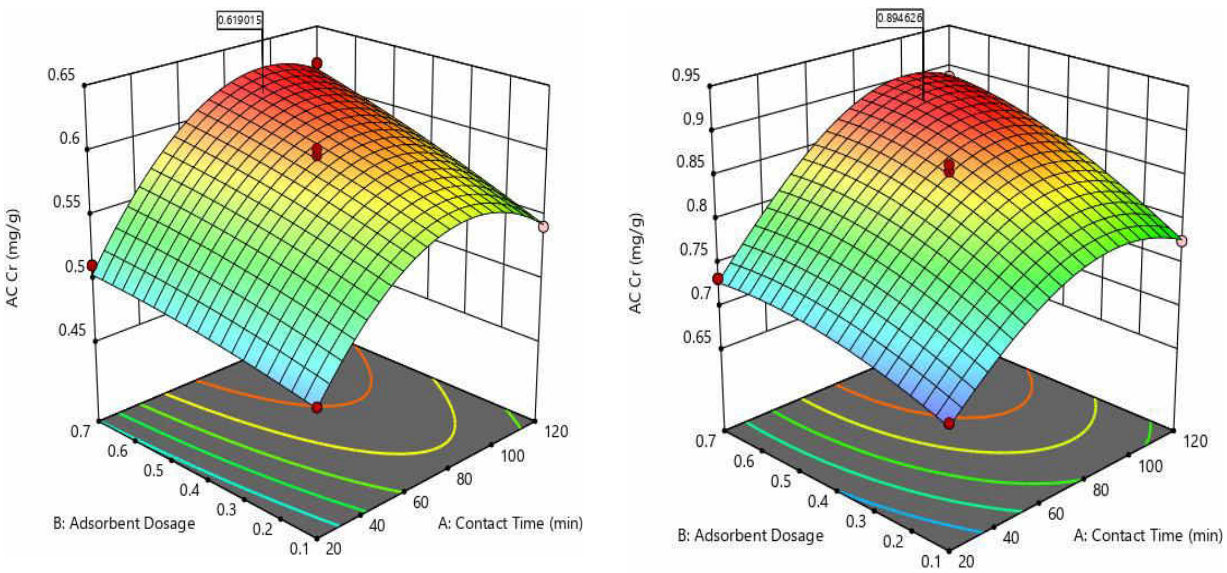

Figure 9. 3D response surface plot for the adsorption of Cr (V) ions on SCB (left) and LM (right).

In analyzing the objective functions in relation to the optimal operating conditions of the biosorption system, the variation of the process parameters were considered (independent variables) and the influence on the previously established experimental field, provided that the biosorption capacity (q, mg/g) are maximized. The primary goal of the response surface is to efficiently track the optimum values of variables, maximizing the response. Through the analysis of the plots, the best response range can be calculated. Each response plot represents an infinite number of combinations of two test variable with the other maintained constant [33]. Analyzing the 3D plots, the quantities of Cr (VI) adsorbed by SCB, LM and their blend per unit gram were 0.61, 0.89 and 1.56 mg/g, respectively.

Lemongrass demonstrated a greater absorption of Cr (VI) ions compared to sugarcane bagasse, attributed to the higher affinity of Cr (VI) ions towards the biosorbent. Significantly, the blend displayed enhanced performance, surpassing the individual materials, which indicates improved affinity for Pb (II) ions when the materials are combined. The plots show the optimal conditions for the adsorption of Cr (VI) ions from textile wastewater, using SCB, LM and their blend are observed at a contact time of 82, 69 and 71 min, respectively and at an adsorbent dosage of 0.62, 0.58 and 0.45 g. A desirability value of 1.00, 0.821 and 1.00 was obtained after optimizing both process variables i.e. contact time and adsorbent dosage. The

desired objective of this numerical optimization was to maximize the adsorption capacity too. The effect of contact time on the adsorption capacity of Cr (VI) using SCB, LM and their blend was studied within the range 20-120 min and the results presented in Figures 9 and 10 were analyzed. It shows that the adsorption of Cr (VI) using SCB increased with an increase in contact time and then slightly decreased after equilibrium was attained at 82 min of agitation. Subsequently, a decline in the adsorption capacity was observed.

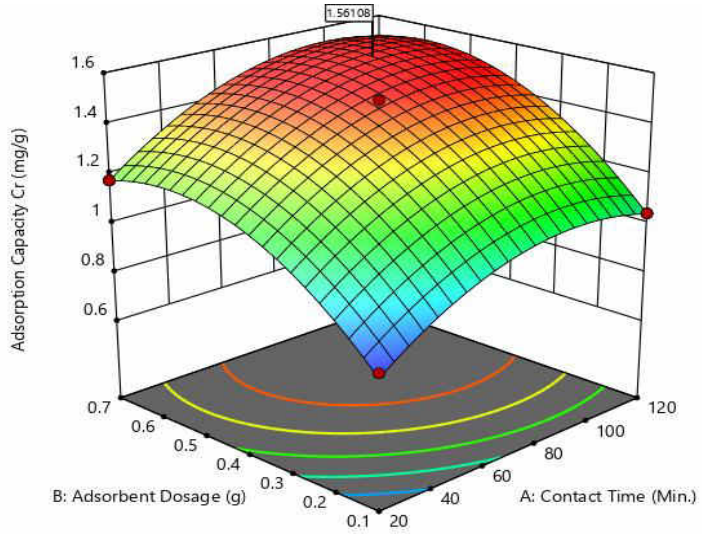

Figure 10. 3D response surface plot for the adsorption of Cr (VI) ions onto a blend derived from SCB and LM.

Similarly, using LM as a biosorbent for the adsorption of Cr (VI) ions, the adsorption capacity increased with an increase in contact time and then slightly decreased after which equilibrium was attained at 70 min of agitation. Subsequently, a decline in the adsorption capacity was observed. For the adsorption of Cr (VI) ions using the blend derived from SCB and LM, the adsorption capacity of Cr (VI) ions increased rapidly with an increase in contact time, reaching equilibrium at 71 min of agitation, however, beyond this point, there was no substantial change observed with further increase with time. This finding aligns with the result reported by [13, 20, 34, 35]. This trend may be attributed to the large number of vacant sites available at the beginning of the process, which eventually become saturated, resulting in a constant adsorption capacity. After attaining equilibrium, the adsorption process may slow down because of the saturation of binding sites on the adsorbent surface [36]. Generally, the uptake of metal increased with an increase in contact time and then ceased due to the saturation of the binding sites on the cell surface [37].

The effect of adsorbent dosage on the adsorption of Cr (VI) using SCB, LM, and their blend was studied by varying the dosage from 0.1 to 0.7 g, as illustrated in Figures 9 and 10. For the adsorption of Cr (VI) ions using SCB, it was observed that adsorption capacity increases with an increase in adsorbent dosage until an optimum dosage was reached at 0.62 g. Similarly, the adsorption of Cr (VI) ions using LM increases with an increase in the amount of adsorbent dosage until an equilibrium dosage is attained at 0.58. The adsorption capacity of Cr (VI) increases over time, reaching a plateau at an equilibrium dosage of 0.45 g, and then becoming constant with no notable changes observed upon increasing the dosage. This increase could be attributed to the overall increase in the surface area of the biosorbent, which in turn increased the number of available binding sites for adsorption [38]. However, as the initial adsorbent dose increases and the number of active sites for ion binding increases, providing easier penetration of metal into the active sites and consequently, the

resultant adsorption also increases, and after a certain value, the increase of the amount of the adsorbent does not affect the adsorption process because of saturation of active sites [39]. A similar results were reported by [1, 13, 19].

3.3. *Adsorption Isotherm and Kinetic Models*

The experimental data were fitted into the non-linear isotherms and kinetic models employed for this study, employing a non-linear curve fitting tool in OriginPro 9 software. In each case, the best model considered was the one with the highest correlation coefficient R^2 and lowest chi-square X^2 values. The closer the R^2 values are to unity, the higher the goodness of fit, and the lower the Chi-square values, the better the fit [14].

3.3.1. Adsorption Isotherms

The isotherm parameters, as well as the correlation coefficients (R^2) and chi-square (X^2) values derived from Figure 11 for the adsorption isotherms of Cr (VI) ions using SCB, as shown in Table 3, indicating that all three models fit the experimental data. The Langmuir isotherm offers the best fit among the models, with low reduced chi-square values of 0.00027 for Cr (VI) ions, and large adjusted R^2 values of 0.9873. This suggests that the Langmuir isotherm is more suitable for describing the adsorption of Cr (VI) ions using sugarcane bagasse than the other two isotherm models. This implies that Cr (VI) ions adsorption follows the monolayer adsorption, in which all metal binding sites have the same energy levels and there are no interactions between the adsorbed metals, nor is there any transmigration of sorbate within the surface area plane [40]. Similar results were reported by Pagala on the adsorption of Pb (II) and Cr (VI) ions using sugarcane bagasse [41]. Additionally, Kumar et al. reported similar results for the adsorption of Cr (VI) ions onto groundnut shells [42].

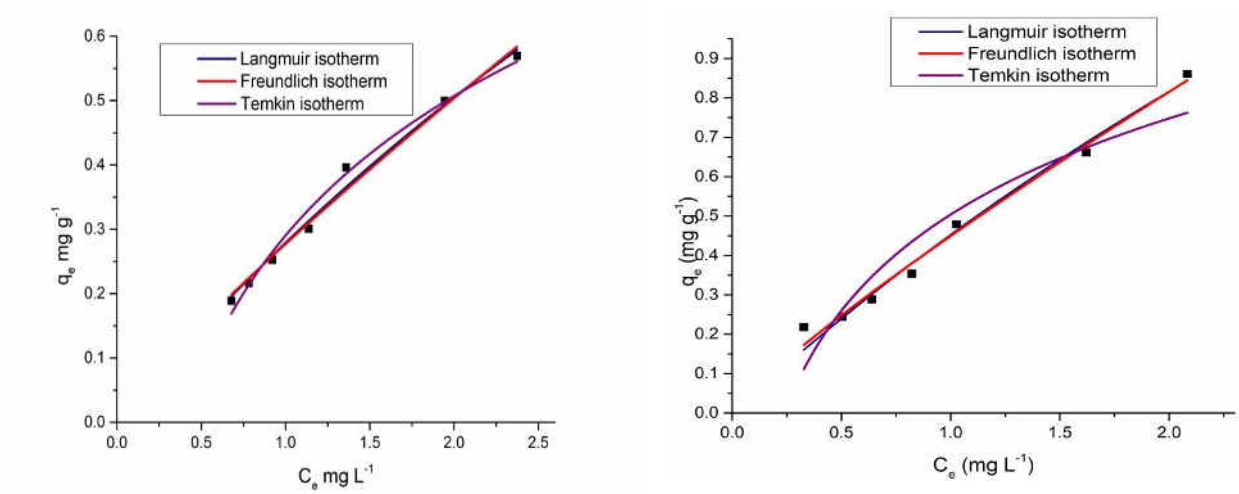

Figure 11. Non-linear models for the adsorption isotherm of Cr (VI) ions using SCB (left) and LM (right).

The maximum adsorption capacities for Cr (VI) ions were estimated using Langmuir isotherm and were found to be 2.68 mg/g, with a Langmuir constant of 0.1160 L/mg. The dimensionless separation factor R_L is used to analyze the adsorption process's favorability, with Cr (VI) values of 0.7455. These values describe a favorable adsorption isotherm. The R_L values indicate the order of isotherm: R_L>1signifies an unfavorable isotherm, R_L=1 indicates linear isotherm, R_L<1 denotes favorable isotherm while R_L=0 signifies an irreversible isotherm [43].

Similarly, the adsorption isotherm parameters reported in Table 3 show that Cr (VI) biosorption follows the Freundlich isotherm as evident by higher values of R^2 (0.9858) and

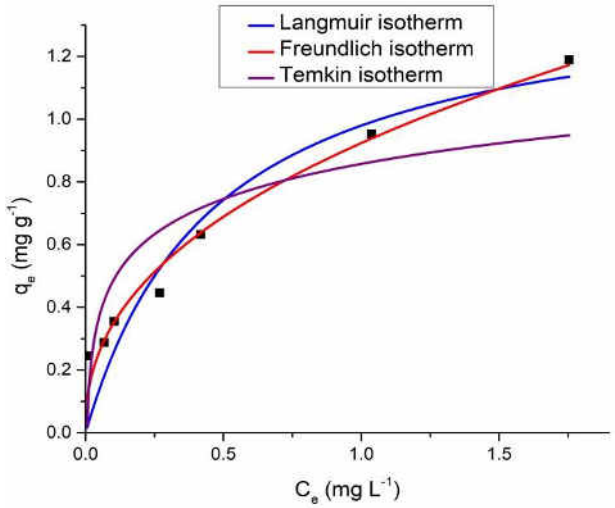

Figure 12. Non-linear models for the adsorption isotherm of Cr (VI) using a blend derived from sugarcane bagasse and lemongrass.

lower reduced chi-square (0.00082) values when compared to other isotherms. It means that the fitted model followed heterogeneous and multilayer adsorption of Cr (VI) ions on the surface of the LM. The findings were consistent with those previously reported by El Dean et al.'s work on Cr (VI) ions adsorption on SCB [20]. The maximum adsorption capacities (q_m), for Cr (VI) ions were estimated using Langmuir and found to be 4.153 mg/g, as indicated in Table 3. The separation factor R_L ranges from 0 to 1, indicating favorable biosorption of Cr (VI) ions on LM with values 0.7355. The R_L values imply that Langmuir adsorption is reversible (R_L=0), favorable (0<R_L<1), linear (R_L=1) or unfavorable (R_L>1) [17].

Table 3

Adsorption isotherm constants for adsorption of Cr (VI) ions

	Biosorbent	Q_m $(\frac{mg}{g})$	K_L $(\frac{L}{mg})$	R^2	X^2
Langmuir	SCB	2.6750	0.1160	0.9873	0.00027
	LM	4.153	0.1222	09813	0.001
	Blend	1.4397	2.1289	0.8698	0.0169
		^{1}/n	K_f $(\frac{mg}{g})$	R^2	X^2
Freundlich	SCB	0.8630	0.2760	0.9835	0.00035
	LM	0.8601	0.4492	0.9858	0.00082
	Blend	0.4246	0.9237	0.9679	0.0055
		b $(\frac{J}{mol})$	$K_T(\frac{L}{g})$	R^2	X^2
Temkin	SCB	3.195	2.526	0.9852	0.00032
	LM	2.838	4.1776	0.8867	0.0065
	Blend	6.1777	3.1396	0.6954	0.0396

Note: Q_m = maximum monolayer adsorption capacity; K_L = Langmuir Constant; K_f = Freundlich constant; R^2= correlation coefficient; X^2= Chi square; n is the adsorption intensity; K_T binding energy; b = heat of adsorption; L = Liter; mg/g = Milligram per gram; J/mol = joule per mole.

For the blend material, the reduced chi-square and adjusted correlation coefficient (R^2) values obtained from Figure 12 for Cr (VI) ions adsorption using a blend formed from SCB and LM, as shown in Table 3, indicate that all three models show a good fit with the experimental data. Freundlich shows the best fit with a higher R^2 value of 0.9679 and a low reduced chi-square 0.0055. This shows that the Freundlich isotherm is more suitable for describing the

adsorption of Cr (VI) ions. This implies the fitted model followed heterogeneous and multilayer adsorption of Cr (VI) ions on the surface of the adsorbent. Similar results were previously reported by [20] in their work on the adsorption of Cr (VI) ions on SCB. The maximum adsorption capacities (q_m), as calculated by Langmuir were determined to be 1.4397 mg/g Cr (VI) ions, as shown in Table 3. The dimensionless separation factor R_L as indicated in Table 3, falls within the range of 0-1, showing favorable Cr (VI) ions biosorption on the blend derived from SCB and LM, with values 0.1376. The value of R_L indicates the type of isotherm to be either unfavorable (R_L>1), linear (R_L=1), favorable (0<R_L<1) or irreversible (R_L=0) [20]. The Temkin isotherm has the least fit among the three isotherms as shown in Table 3 for Cr (VI) adsorption using SCB, LM and their blend.

3.3.2. Adsorption Kinetics

To further understand the adsorption mechanism of Cr (VI) on SCB, LM and their blend, the kinetic models used in this work were applied to the experimental data. Non-linear fits of these models are illustrated in Figures 13 and 14, while Table 4 presents the parameters obtained from the model fits.

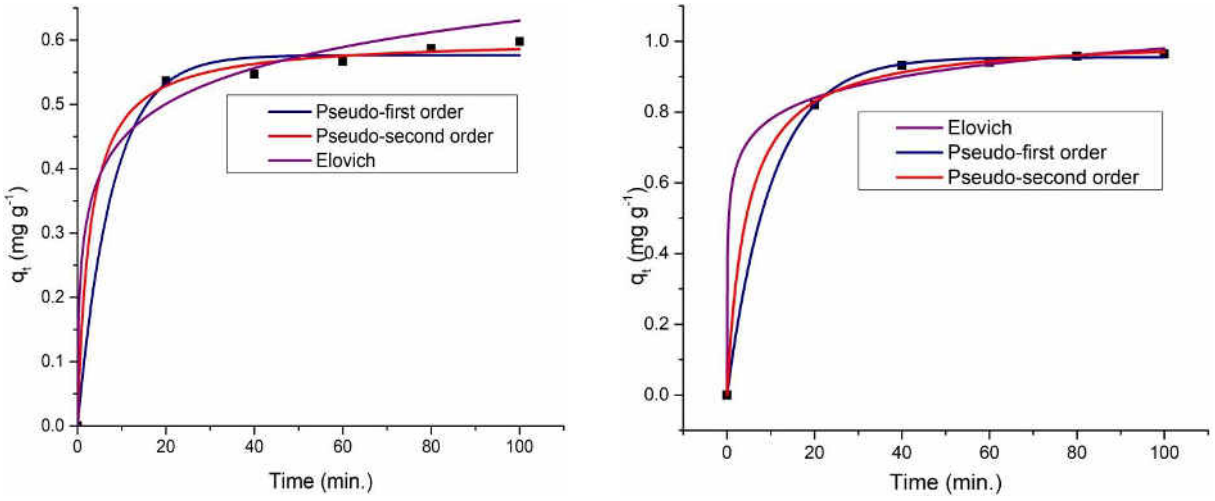

a) b)

Figure 13. Non-linear adsorption kinetics models applied for the adsorption of Cr (VI) ions onto SCB (a) and LM (b).

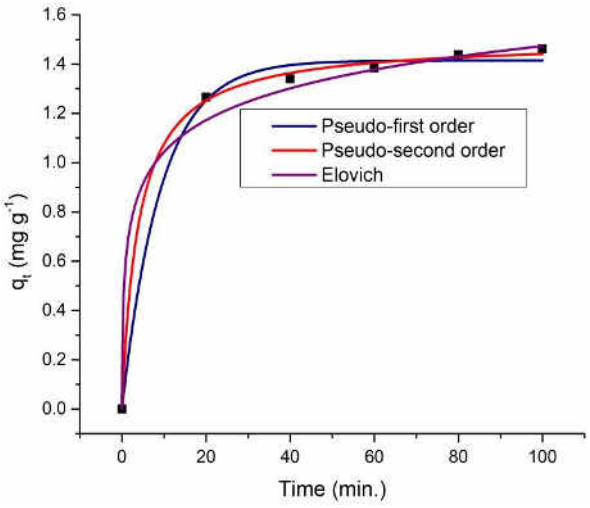

Figure 14. Non-linear adsorption kinetics models applied for the adsorption of Cr (VI) onto a blend derived from sugarcane bagasse and lemongrass.

The parameters extracted from Figure 13 and presented in Table 4 reveal that the correlation coefficient R^2 and reduced chi-square X^2 values for PFO, PSO, and Elovich kinetic models indicate that all kinetic models showed a good fit. However, for Cr (VI) ions adsorption using SCB, the PSO, exhibiting the highest correlation coefficient of 0.9975 for Cr (VI), which is closer to unity, shows a better fit. This model predicts an equilibrium Cr (VI) ions uptake of 0.57655 mg/g, which is in agreement with the experimentally obtained value of 0.62 mg/g. The PSO kinetic model shows the best fit with the adjusted R^2 value of 0.9996, along with a low chi-square value of 0.00013 for Cr (VI) ions adsorption using LM. This model predicts an equilibrium uptake of 1.01404 mg/g for Cr (VI), closely aligning with experimentally obtained values.

Table 4

Adsorption kinetic model constants for Cr (VI) ions

	Biosorbent	K_1	Q_e	Q_p	R^2	X^2
PFO	SCB	0.1286	0.62	0.576	0.9939	0.0003
	LM	0.097	0.89	0.954	0.9991	0.0006
	blend	0.108	1.49	1.414	0.9947	0.0017
	Biosorbent	K^2	Q_e	Q_p	R^2	X^2
PSO	SCB	0.595	0.62	0.602	0.9975	0.00013
	LM	0.220	0.89	1.014	0.9996	0.0001
	Blend	0.1699	1.49	1.498	09987	0.0004
	Biosorbent	A	β	-	R^2	X^2
Elovich	SCB	2.001	12.402	-	0.9834	0.0009
	LM	69.95	11.53	-	0.9971	0.0004
	Blend	4.904	5.344	-	0.9918	0.00262

Note: Q_e = experimental adsorption capacity; Q_p = predicted adsorption capacity; K_1 = PFO constant; K^2 PSO constant; R^2= correlation coefficient; X^2= Chi-square; L = Liter; mg/g = Milligram per gram; J/mol = joule per mole.

Similarly, the PSO kinetic model exhibits adjusted R^2 values of 0.09987, along with reduced chi-square values of 0.00043 for Cr (VI) ions adsorption using the blend material. This model predicts equilibrium Cr (VI) ions uptake of 1.497 mg/g which closely aligns with the experimentally obtained value of 1.49 mg/g. The closer the R^2 value is to unity, the better the fit. Notably, The PSO stands out as the best fit among the three models tested (in Figures 13 and 14) for Cr (VI) ions adsorption using SCB, LM, and their blend, implying that the active sites on the adsorbent surface significantly influence the adsorption capacity. The findings obtained were in good agreement with previous studies, which also reported that the adsorption process of Cr (VI) ions followed the PSO kinetic model following the literature [41, 42 ,44, 45].

4. Conclusions

This study has demonstrated the significant potential of sugarcane bagasse (SCB) and lemongrass (LM) as effective biosorbents for the removal of chromium (VI) ions from textile wastewater. The results indicate that both materials exhibit substantial adsorption capacities, with their blend demonstrating superior performance. Characterization techniques, including BET analysis and FTIR, provided critical insights into the biosorbents' properties. The BET analysis revealed high surface areas for SCB (501.999 m^2/g), lemongrass (811.761 m^2/g), and their blend (1047.885 m^2/g), which are essential for maximizing adsorption efficiency. The FTIR analysis identified significant functional groups, such as hydroxyl and carbonyl, crucial

for binding Cr (VI) ions, suggesting strong chemical interactions that enhance biosorption effectiveness.

In addition to the characterization results, the kinetic studies showed that the adsorption of Cr (VI) ions followed the Pseudo-second order model for all biosorbents, indicating that the process is significantly influenced by the availability of active sites on the adsorbent surfaces. This model's high correlation coefficients suggest that chemisorption is the dominant mechanism for Cr (VI) ions uptake. Moreover, isotherm analysis revealed that the Langmuir isotherm provided the best fit for SCB, indicating monolayer adsorption on homogeneous sites, while the Freundlich isotherm was more appropriate for lemongrass and the blend, suggesting heterogeneous and multilayer adsorption. These findings highlight the complexity of the interactions between the biosorbents and chromium (VI) ions, underscoring the diverse mechanisms involved in the adsorption process.

Overall, the findings of this research contribute significantly to the understanding of biosorption technology and promote the use of sustainable materials in wastewater treatment processes. SCB and LM emerge as viable options for the remediation of chromium (VI) ions, paving the way for further investigations into their application for other heavy metals. This study encourages a shift towards environmentally friendly practices in wastewater management, reinforcing the potential of natural biosorbents in mitigating pollution and protecting water resources.

Conflicts of Interest: The author declares no conflict of interest.

References

1. Balarak, D.; Jaafari, J.; Hassani, G. The use of low-cost adsorbent (Canola residues) for the adsorption of methylene blue from aqueous solution: Isotherm, kinetic and thermodynamic studies. *Colloids and Interface Science Communications* 2015, 7, pp. 16-19.
2. Ameen, H.S.A.; Yub, H.N.; Mahmoud, N.M.; Al-Fakih, A.; Abdulhakim, S.G.A.; Kolawole, A.H. Removal of cadmium from aqueous solution by optimized rice husk biochar using response surface methodology. *Ain Shams Engineering Journal* 2022, 13(1), pp. 101516.
3. Rizvi, A.; Ahmed, B.; Zaidi, A.; Khan, M.S. Biosorption of heavy metals by dry biomass of metal tolerant bacterial biosorbents: an efficient metal clean-up strategy. *Environ Monit Assess.* 2020, 192, pp.1-21
4. Oyegoke, T.; Adnan, A. Impact of Selected Adsorbent Functional Groups on Chromium Sorption Capacities In An Effluent Treatment: A DFT Study. *The Journal of Engineering Research* [TJER] 2024, 21(1), pp. 59-70.
5. Zhao, Y.; Yang, S.; Ding, D.; Effective adsorption of Cr (VI) from aqueous solution using natural Akadama clay. *J Colloid Interface Sci.* 2013, 395, pp. 198-204.
6. Agarwal, A.; Upadhyay, U.; Sreedhar, I.; Singh, S.A.; Patel, C.M. A review on valorization of biomass in heavy metal removal from wastewater. *Journal of Water Process Engineering* 2020, 38, p.101602.
7. Oyegoke, T.; Igwebuike, C.M.; Oyegoke, A. Unraveling the influence of biomaterial's functional groups in Cd biosorption: a density functional theory calculation. *Pure and Applied Chemistry* 2024, 96(3), pp. 399-412.
8. Sen, S.; Nandi, S.; Dutta, S. Application of RSM and ANN for optimization and modeling of biosorption of chromium (VI) using cyanobacterial biomass. *Appl Water Sci.* 2018, 8, pp.1-12.
9. Yous, R.; Mohellebi, F.; Cherifi, H.; Amrane, A. Competitive biosorption of heavy metals from aqueous solutions onto Streptomyces rimosus. *Korean Journal of Chemical Engineering* 2018, 35, pp.890-899.
10. Abdelfattah, I.; Ismail, A.A.; Sayed, F.; Almedolab, A.; Aboelghait, K.M. Biosorption of heavy metals ions in real industrial wastewater using peanut husk as efficient and cost-effective adsorbent. *Environ Nanotechnol Monit Manag.* 2016, 6, pp.176-183.
11. Martini, S.; Afroze, S.; Ahmad, R.K. Modified eucalyptus bark as a sorbent for simultaneous removal of COD, oil, and Cr(III) from industrial wastewater. *Alexandria Engineering Journal* 2020, 59(3), pp.1637-1648.
12. Molaudzi, N.R.; Ambushe, A.A.; Sugarcane Bagasse and Orange Peels as Low-Cost Biosorbents for the Removal of Lead Ions from Contaminated Water Samples. *Water*, 2022, 14(21), p.3395.

13. Aminu, Z.I.; Galadima, M.S.; Isa, M.T.; Ameh, A.O.; Sanni, M.I. Application of Response Surface Methodology in Adsorption of Lead Ion from Laboratory Simulated Wastewater Using Eucalyptus Tereticornis Leaves. *Nigerian J. Mater. Sci. Eng.* 2016, 6(1), pp. 1-10.
14. Ezeonuegbu, B.A.; Machido, D.A.; Whong, C.M.Z. Agricultural waste of sugarcane bagasse as efficient adsorbent for lead and nickel removal from untreated wastewater: Biosorption, equilibrium isotherms, kinetics and desorption studies. *Biotechnology Reports* 2021, 30, pp. e00614.
15. Homagai, P.L.; Ghimire, K.N.; Inoue, K. Preparation and characterization of charred xanthated sugarcane bagasse for the separation of heavy metals from aqueous solutions. *Separation Science and Technology* 2010, 46(2), pp. 330-339.
16. Aruna-Bagotia, N.; Sharma, A.K.; Kumar, S. A review on modified sugarcane bagasse biosorbent for removal of dyes. *Chemosphere* 2021, 268, pp. 129309.
17. Babarinde, A.; Ogundipe, K.; Sangosanya, K.T.; Akintola, B.D.; Hassan, E. Comparative study on the biosorption of Pb(II), Cd(II) and Zn(II) using Lemon grass (Cymbopogon citratus): Kinetics, isotherms and thermodynamics. *Chem. Int.* 2016, 2(2), pp. 89-102.
18. Zein, R.; Satrio-Purnomo, J.; Ramadhani, P.; Safni-Alif, M.F.; Putri, C.N. Enhancing sorption capacity of methylene blue dye using solid waste of lemongrass biosorbent by modification method. *Arabian Journal of Chemistry* 2023, 16(2), pp. 104480.
19. Silva, C.E.; Gama, B.M.V.; Gonçalves, A.H.; Medeiros, J.A.; Abud, A.K.S. Basic-dye adsorption in albedo residue: Effect of pH, contact time, temperature, dye concentration, biomass dosage, rotation, and ionic strength. *Journal of King Saud University - Engineering Sciences* 2020, 32(6), pp. 351-359.
20. Kamal-El-Dean, A.M.; Hashem, E.Y.; Ahmed, M.M.; Mohamed, M.A.; Hussain, S.M. Removal of chromium(VI) from wastewater using citric acid modified sugarcane bagasse. *European Chemical Bulletin* 2019, 8(5), pp. 141-149.
21. Darweesh, M.A.; Elgendy, M.Y.; Ayad, M.I.; Ahmed, A.M.M.; Elsayed, N.M.K.; Hammad, W.A. Adsorption isotherm, kinetic, and optimization studies for copper (II) removal from aqueous solutions by banana leaves and derived activated carbon. *S Afr J Chem Eng.* 2022, 40, pp. 10-20.
22. Sahoo, T.R.; Prelot, B. Adsorption processes for the removal of contaminants from wastewater: the perspective role of nanomaterials and nanotechnology. *Micro and Nano Technologies* 2020, pp. 161-222.
23. Dwiyaniti, M.; Elang-Barruna, A.G.; Muhamad-Naufal, R.; Subiyanto, I.; Setiabudy, R.; Hudaya, C. Extremely high surface area of activated carbon originated from sugarcane bagasse. *IOP Conf Ser Mater Sci Eng.* 2020, 909(1), 012018.
24. Darla, U.R.; Lataye, D.H.; Kumar, A.; Pandit, B.; Ubaidullah, M. Adsorption of phenol using adsorbent derived from Saccharum officinarum biomass: optimization, isotherms, kinetics, and thermodynamic study. *Sci Rep.* 2023, 13(1), 18356.
25. Ogundeji, O.J.; Jimoh, A. Characterization of sugarcane bagasse as a potential treatment of heavy metal effluents by the response surface methodology. *Int. J. Pure Appl. Sci.* 2021, 20(9), pp. 1-24.
26. Ahmad, M.A.; Ahmed, N.B.; Adegoke, K.A.; Bello, O.S. Sorption studies of methyl red dye removal using lemon grass (Cymbopogon citratus). *Chemical Data Collections* 2019, 22, 100249.
27. Harripersadth, C.; Musonge, P.; Makarfi-Isa, Y.; Morales, M.G.; Sayago, A. The application of eggshells and sugarcane bagasse as potential biomaterials in the removal of heavy metals from aqueous solutions. *S Afr J Chem Eng.* 2020, 34(1), pp. 142-150.
28. Bernal-Jácome, L.A.; Olvera-Izaguirre, L.; García, M.G.; Delgado-Delgado, R.; Rodríguez, M.Á.E. Adsorption of Lead (II) from Aqueous Solution Using Adsorbents Obtained from Nanche Stone (Byrsonima Crassifolia). *J Mex Chem Soc.* 2021, 64(4), pp. 301-315.
29. Lee, L.Y.; Lee, X.J.; Chia, P.C.; Tan, K.W.; Gan, S. Utilisation of Cymbopogon citratus (lemon grass) as biosorbent for the sequestration of nickel ions from aqueous solution: Equilibrium, kinetic, thermodynamics and mechanism studies. *J Taiwan Inst Chem Eng.* 2014, 45(4), pp. 1764-1772.
30. Abdolali, A.; Ngo, H.H.; Guo, W. Characterization of a multi-metal binding biosorbent: Chemical modification and desorption studies. *Bioresour Technol.* 2015, 193, pp. 477-487.
31. Isam, M.; Baloo, L.; Chabuk, A.; Majdi, A.; Al-Ansari, N. Optimization and modelling of Pb (II) and Cu (II) adsorption onto red algae (Gracilaria changii)-based activated carbon by using response surface methodology. *Biomass Convers Biorefin.* 2024, 14(15), pp. 16799-16818.
32. Amini, M.; Younesi, H.; Bahramifar, N. Application of response surface methodology for optimization of lead biosorption in an aqueous solution by *Aspergillus niger*. *J Hazard Mater* 2008, 154(1-3), pp. 694-702.

33. Fertu, D.I.; Dragoi, E.N.; Bulgariu, L.; Curteanu, S.; Gavrilescu, M. Modeling the Biosorption Process of Heavy Metal Ions on Soybean-Based Low-Cost Biosorbents Using Artificial Neural Networks. *Processes* 2022, 10(3), 603.
34. Amode, J.O.; Santos, J.H.; Alam, Z.; Mirza, A.H.; Mei, C.C. Adsorption of methylene blue from aqueous solution using untreated and treated (Metroxylon spp.) waste adsorbent: equilibrium and kinetics studies. *International Journal of Industrial Chemistry* 2016, 7, pp. 333-345.
35. Kerrou, M.; Bouslamti, N.; Raada, A.; Elanssari, A.; Mrani, D.; Slimani, M.S. The Use of Sugarcane Bagasse to Remove the Organic Dyes from Wastewater. *Int J Anal Chem.* 2021, 1, 5570806.
36. Ashfaq, A.; Nadeem, R.; Bibi, S. Efficient adsorption of lead ions from synthetic wastewater using agrowaste-based mixed biomass (Potato peels and banana peels). *Water* 2021, 13(23), 3344.
37. Hauwa, H.; Whong, .C.M.Z.; Ado, S.A.; Abdulmumin, A.N. Optimization of Culture Condition for Biosorption of Lead using Pseudomonas aeruginosa isolated from Gold Mining Site of Anka, Zamfara State. *Journal of Microbiology Research* 2020, 5(1), pp. 43-48.
38. Al-Homaidan, A.A.; Alabdullatif, J.; Al-Hazzani, A.A.; Al-Ghanayem, A.A.; Alabbad, A.F. Adsorptive removal of cadmium ions by Spirulina platensis dry biomass. *Saudi J Biol Sci.* 2015, 22(6), pp. 795-800.
39. Kaya, N.; Arslan, F.; Yildiz Uzun, Z. Production and characterization of carbon-based adsorbents from waste lignocellulosic biomass: their effectiveness in heavy metal removal. *Fullerenes Nanotubes and Carbon Nanostructures*, 2020, 28(10), pp. 769-780.
40. Kalantari, K.; Ahmad, M.B.; Masoumi, H.R.F.; Shameli, K.; Basri, M.; Khandanlou, R. Rapid adsorption of heavy metals by Fe3O4/talc nanocomposite and optimization study using response surface methodology. *Int J Mol Sci 2014*, 15(7), pp. 12913-12927.
41. Pagala, B. Biosorption of Chromium and Lead from Electroplating Industry Effluent Using Modified Cane Bagasse. *Journal of The Institution of Engineers* 2023, 1, pp. 1-12.
42. Kumar, H.; Kumara Jawa, G.; Rai, A. Removal of Cr(VI) using citric acid and phosphoric acid-modified groundnut shells. *IJCCE* 2024, 43(3), pp. 1045-1059.
43. Naseem, K.; Huma, R.; Shahbaz, A. Extraction of Heavy Metals from Aqueous Medium by Husk Biomass: Adsorption Isotherm, Kinetic and Thermodynamic study. *Zeitschrift fur Physikalische Chemie* 2019, 233(2), pp. 201-223.
44. El Yakoubi, N.; El Ansari, Z.N.; Ennami, M.; El Kbiach, M.L.; Bounab, L.; El Bouzdoudi, B.; Biosorption of Hexavalent Chromium Cr(VI) onto Ziziphus Lotus Fruits Powder: Kinetics, Equilibrium, and Thermodynamics. *Journal of Ecological Engineering* 2024, 25(2), pp. 321-332.
45. Mousavi, S.A.; Almasi, A.; Navazeshkh, F.; Falahi, F. Biosorption of lead from aqueous solutions by algae biomass: optimization and modeling. *Desalination Water Treat.* 2019, 148, pp. 229-237.

Citation: Dangamba, A.S.; Oyegoke, T.; Ocheje, F.E.; Dikko, M.A.; Galadima, M.S. Evaluating the adsorption potential of sugarcane bagasse and lemongrass for chromium (VI) removal in wastewater treatment. *Journal of Engineering Science* 2024, XXXI (3), pp. 96-116. https://doi.org/10.52326/jes.utm.2024.31(3).09.

Submission of manuscripts: jes@meridian.utm.md